Journal of Power Sources 222 (2013) 237–242

Contents lists available at SciVerse ScienceDirect

Journal of Power Sources

journal homepage: www.elsevier.com/locate/jpowsour

All-solid-state Li–sulfur batteries with mesoporous electrode and thio-LISICON solid electrolyte

Miki Nagao [a], Yuki Imade [a], Haruto Narisawa [a], Takeshi Kobayashi [a], Ryota Watanabe [b], Toshiyuki Yokoi [b], Takashi Tatsumi [b], Ryoji Kanno [a,*]

[a] Department of Electronic Chemistry, Tokyo Institute of Technology, Yokohama 226-8502, Japan
[b] Chemical Resources Laboratory, Tokyo Institute of Technology, Yokohama 226-8502, Japan

HIGHLIGHTS

► All-solid-state battery with a composite cathode, sulfur/CMK-3, and solid electrolyte, thio-LISICON was studied.
► CMK-3 is a high ordered two-dimensional meso-porous carbon and provides a framework structure for the cathode composite.
► The sulfur/CMK-3 cathode exhibited high capacity and excellent cycling characteristics.

ARTICLE INFO

Article history:
Received 23 May 2012
Received in revised form
4 August 2012
Accepted 14 August 2012
Available online 3 September 2012

Keywords:
Lithium secondary battery
Sulfur
All-solid-state battery
Carbon
CMK-3
Mesoporous carbon

ABSTRACT

All-solid-state lithium–sulfur batteries were developed using elemental sulfur as a positive electrode, Li–Al alloy as a negative electrode, thio-LISICON as a solid electrolyte, and mesoporous carbon (CMK-3) as the framework for the positive electrode. The mesoporous framework provided high electrical conduction and improved electrode utilization. The sulfur provided a high reversible capacity and high current charge discharge characteristics. Sulfur introduced into the pore structure of the mesoporous carbon interacts with edges of the graphene sheet and both the sulfur and graphene layers participate in a highly reversible reaction.

1. Introduction

High-capacity rechargeable batteries are promising power storage devices for future portable electronic devices and electric vehicles. Batteries with lithium-based systems have high energy densities, are lightweight, and have low electrochemical potentials. Sulfur positive electrodes in lithium-based systems have a theoretical capacity of 1672 mAh g^{-1}, which is 10 times higher than that of conventional $LiCoO_2$ positive electrodes. This theoretical capacity is based on the charge–discharge reaction, $S + 2Li^+ + 2e^- \leftrightarrow Li_2S$. Due to the abundance of elemental sulfur, batteries based on the lithium/sulfur redox couple have the potential to be inexpensive in addition to being safe and having high energy densities. However, the low electrical conductivity of sulfur (5×10^{-30} S cm^{-1} at room temperature [1]) results in relatively low utilization of the active materials in sulfur electrodes [2,3]. During charging and discharging, sulfur is converted into polysulfides, which are soluble in liquid organic electrolytes; this loss of the active material in liquid electrolytes leads to poor rechargeability. This problem needs to be overcome in future lithium–sulfur batteries [4,5].

Mesoporous carbon consists of a carbon matrix with mesopores [6–9]. These pores have two-dimensional (e.g., CMK-3) or three-dimensional (e.g., carbon replica) arrangements. CMK-3 synthesized from a template of SiO_2 (SBA-15) powder [6,10] has a two-dimensional ordered structure consisting of a hexagonal arrangement of cylindrical rods. As CMK-3 exhibits a high electrical conductivity [7], ordered mesopores may provide a new electrode structure for lithium–sulfur batteries that has the potential to realize close contact between the electrode and the electrolyte and a high electrical conduction in the electrode matrix [11,12].

* Corresponding author. Tel./fax: +81 045 924 5401.
E-mail address: kanno@echem.titech.ac.jp (R. Kanno).

0378-7753/$ – see front matter
http://dx.doi.org/10.1016/j.jpowsour.2012.08.041

Since all-solid-state batteries are more stable and safer than batteries that employ liquid electrolytes, they have the potential to be used as ultra-high energy density systems. Furthermore, an all-solid-state configuration can realize close solid–solid contact, which prevents the dissolution of polysulfides formed by the electrode reaction in lithium–sulfur systems. The non-inflammability of solid electrolytes permits an extremely high capacity to be realized. The solid electrolyte thio-LISICON ($Li_{3.25}Ge_{0.25}P_{0.75}S_4$) exhibits a high ionic conductivity of (2–4) $\times$ 10^{-3} S cm^{-1} at room temperature, which is comparable to those of liquid electrolytes [13,14]. However, all-solid-state batteries suffer from a high interfacial resistance at the SE/electrode interface. We previously reported that a sulfur/acetylene black (AB) composite can enhance the reversibility of the charge–discharge characteristics. This composite structure was formed by mixing elemental sulfur vapor and AB [15]. AB has a random network of macropores between its constituent particles and it has a low Brunauer–Emmett–Teller (BET) surface area. Using an electrode structure with a framework of CMK-3 greatly enhanced the electrode/electrolyte contact and improved the electrical conduction and hence the charge–discharge characteristics [16].

The present study investigates a new electrode structure with the aim of improving the characteristics of all-solid-state lithium–sulfur batteries. The reaction mechanism of a composite electrode consisting of sulfur and the mesoporous carbon, CMK-3, was examined. The composite electrode structure improved sulfur utilization for the charge–discharge capacities and it can thus be used to produce all-solid-state Li–sulfur batteries with high energy densities.

2. Experimental

CMK-3 was synthesized from a template of mesoporous silica SBA-15 [6,10]. The CMK-3/SiO_2 composite was also used as a reference for the composite electrode. The sulfur–carbon composite was prepared by gas-phase mixing, as reported previously [15]. The mixing processes are as follows. Sulfur (Kojundo Chemical Laboratory; >99.99% purity) and CMK-3 or CMK-3 + SiO_2 were weighed in a ratio of 30:70 (weight % (wt.%)), mixed in an argon-filled glove box, sealed in a quartz tube in a vacuum, and then heated at 300 °C. After heating, the tube was slowly cooled to room temperature. The composite was heated for 5 h at 170–230 °C to remove any sulfur outside of the particles. Thio-LISICON ($Li_{3.25}Ge_{0.25}P_{0.75}S_4$) was synthesized by a solid-state reaction and was used as a solid electrolyte [13]. Positive electrodes were fabricated by mixing the sulfur–carbon composite and thio-LISICON with a weight ratio of 50:50 in a planetary ball mill (Fritsch, P-7) for 0.5 h at 380 rpm. The test cell was a polyethylene terephthalate (PET) cylinder with an inner diameter of 10 mm. About 70 mg of the solid electrolyte (thio-LISICON) was pressed into a pellet and 5 mg of the positive electrode was then pressed into one side of the electrolyte pellet at 500 MPa. Lithium–aluminum composites were used for negative electrodes because of their good electrode characteristics for all-solid-state batteries consisting of LiAl and thio-LISICON [17]. The negative electrode was a combination of aluminum foil (thickness: 0.1 mm) and lithium foil (thickness: 0.1 mm; diameter: 10 mm). The Li/Al ratio was about 38/68 mol.%, which provides a potential of 0.38 V vs. Li/Li$^+$. The aluminum foil was attached to the solid electrolyte by applying a pressure of 500 MPa [17] and the lithium sheet was then attached to the aluminum foil. The preparation and fabrication of the cells were performed in a dry (less than 0.1 ppm H_2O) argon-filled glove box (Miwa Mfg. Co. Ltd.). The electrochemical properties were characterized using a multichannel galvanostat (TOSCAT-3100). The charge–discharge current was in the range 0.013–1.3 mA cm^{-2} at 25 °C.

The charge–discharge capacity of the cell was calculated based on the sulfur content of the electrode matrix, which was determined by thermogravimetric analysis (TGA; Rigaku Thermo plus TG8120). The weight ratio of sulfur to carbon in the composite electrode was measured by TGA measurements. TGA measurements were conducted in a helium atmosphere from room temperature to 600 °C at a heating rate of 10 °C min^{-1}. The weight of sulfur in the composite material was determined from the weight loss of the S/C composite material determined by TGA measurements. The ratio of the composite material to the solid electrolyte in the cathode is 50:50 wt.%; the weight of sulfur in the cathode mixture was calculated from this ratio.

The resistivity of the cells was examined by the ac impedance method for frequencies in the range 10 mHz–1 MHz and an applied ac voltage of 10 mV using a Solartron 1260 frequency response analyzer. The electrodes were characterized by X-ray diffraction measurements using a Rigaku Ultima-IV with Cu Kα radiation. Morphologies of the composite electrodes fabricated by gas phase mixing were investigated by field-emission scanning electron microscopy (FE-SEM; Hitachi S-5200). The porosity of the cathode composite was measured by BET measurements with nitrogen gas (BEL JAPAN BELSORP-mini). The pore distribution of carbon was refined by the BJH method [18].

3. Results and discussion

Fig. 1 shows FE-SEM images of CMK-3 and the sulfur/CMK-3 composite after mixing at 300 °C. Mesoscale carbon rods were clearly observed for both samples and no significant changes in the mesoporous structure of the carbon were observed after mixing sulfur and carbon.

The thermal behavior of the sulfur/carbon composite was examined to determine the composite structure of sulfur and the

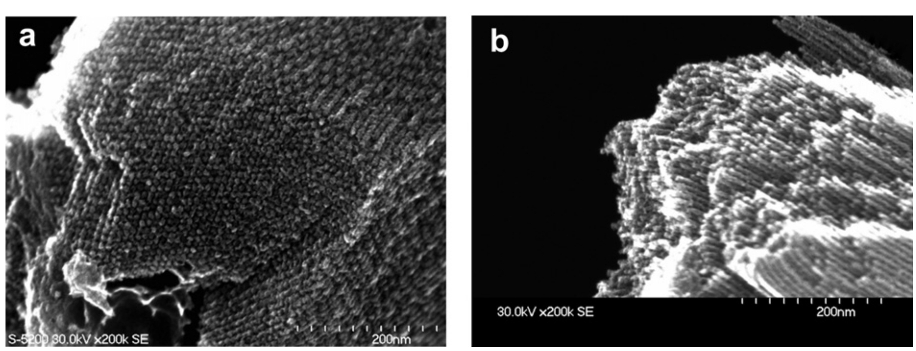

Fig. 1. FE-SEM images of (a) CMK-3 and (b) sulfur/CMK-3 composite.

carbon matrix. Fig. 2 shows TGA curves of CMK-3, the sulfur/CMK-3 composite, and the sulfur/(CMK-3 + SiO_2) composite. No weight changes were observed for the CMK-3 from room temperature to 600 °C, whereas a large reduction in weight at 218 °C was observed for elemental sulfur, which corresponds to evaporation of sulfur. The S/(CMK-3 + SiO_2) composite exhibited a weight loss at 205 °C, which corresponds to removal of sulfur outside the mesopores. As the mesopores in the S/(CMK-3 + SiO_2) composite were filled with SiO_2, the weight reduction was ascribed to evaporation of sulfur deposited outside the mesopore structure. On the other hand, the S/CMK-3 composite exhibited weight losses at two temperatures, 270 and 528 °C, which may correspond to removal of sulfur outside and inside the mesopores in the carbon, respectively.

Fig. 3 shows the results of specific surface area measurements for CMK-3, the S/CMK-3 composite, and the S/CMK-3 composite annealed at 230 °C. The results reveal the pore radius distributions of these three samples. All the samples have pore radius in the range 1–2 nm. No changes were observed in the pore size distribution after mixing with sulfur or heat treatment. However, dV_p/dr_p decreased, indicating a reduction in the surface area on sulfur mixing. This indicates that the pores in the carbon matrix were almost completely filled with sulfur. On heat treatment at 230 °C, dV_p/dr_p increased, indicating an increase in the surface area and a reduction in the amount of sulfur in the pores. Moreover, the shape of the dV_p/dr_p peak of the annealed S/CMK-3 composite is similar to that of the original CMK-3, indicating that the pore surfaces are coated with a thin layer of sulfur. The heat treatment removed sulfur from both inside and outside the mesopores so that closed pores became open. However, the TGA measurements reveal that sulfur is still present in the mesopores. Therefore, sulfur attached to the mesopore walls in the carbon CMK-3 matrix causes the mesopores to open on heat treatment.

Fig. 4 shows charge–discharge curves of a cell with sulfur and CMK-3 composite electrodes with a charge–discharge current density of 0.13 mA cm^{-2}. The cell capacity was calculated based on the sulfur content of the cell. The sulfur/CMK-3 composite electrode has a first discharge capacity of 1600 mAh g^{-1}, which is close to the theoretical capacity of sulfur, indicating that there may be a reaction between lithium and carbon matrix. The charge–discharge curves exhibit only one plateau and the cell voltage during cycling was slightly lower than those of conventional Li/S batteries [11], which also suggests that there is an interaction between lithium and the sulfur/carbon composite matrix. The cell exhibited reversible characteristics and the capacity was above 700 mAh g^{-1} after 10 cycles. In a previous study, we investigated all-solid-state batteries with a composite electrode consisting of sulfur and AB [15]. They had a first discharge capacity of 400 mAh g^{-1}, a reversible capacity of 270 mAh g^{-1}, and a current density of 0.13 mA cm^{-2}. The composite structure of the S/CMK-3 had a higher reversible capacity than elemental sulfur. As large sulfur particles are present outside of the carbon matrix, we tried to reduce these sulfur particles by heat treatment. After heat treatment at 230 °C, the cell with a composite electrode had a first discharge capacity of 3239 mAh g^{-1} based on the sulfur content. After the 20th cycle, the cell still had a reversible capacity of 1300 mAh g^{-1}. The first discharge capacity increased and the reversibility improved remarkably on heat treatment without large sulfur particles. All the charge–discharge curves for the solid state cell exhibit a single plateau; this is different to those for conventional Li/S batteries that generally exhibit two plateaus depending on the reaction products between lithium and sulfur [11]. This indicates that the all-solid-state Li/S cell has a different reaction mechanism from liquid electrolyte Li/S cells. Fig. 5 shows the charge–discharge capacities at 0.09 C as a function of cycle number for composites annealed at various temperatures between 170 and 230 °C. Cells with electrodes that had been annealed at temperatures of 170, 190, 210, and 230 °C have current densities of 0.13, 0.12, 0.058 and 0.023 mA cm^{-2}, respectively. All the C-rate values are 0.09 C. Their capacity increases as the heat treatment temperature is increased from 170 to 230 °C. The first discharge capacity of S/CMK-3(230) was calculated to be 3239 mAh g^{-1} based on the sulfur content in the carbon matrix; this value is about twice the theoretical capacity of sulfur. The capacities after 20 and 50 cycles decreased respectively to 1300 and 1000 mAh g^{-1}, which are still very high. These results indicate that sulfur inside the mesopores participates in reversible charge–discharge reactions. The extremely high capacity, which exceeds the theoretical capacity of sulfur, indicates

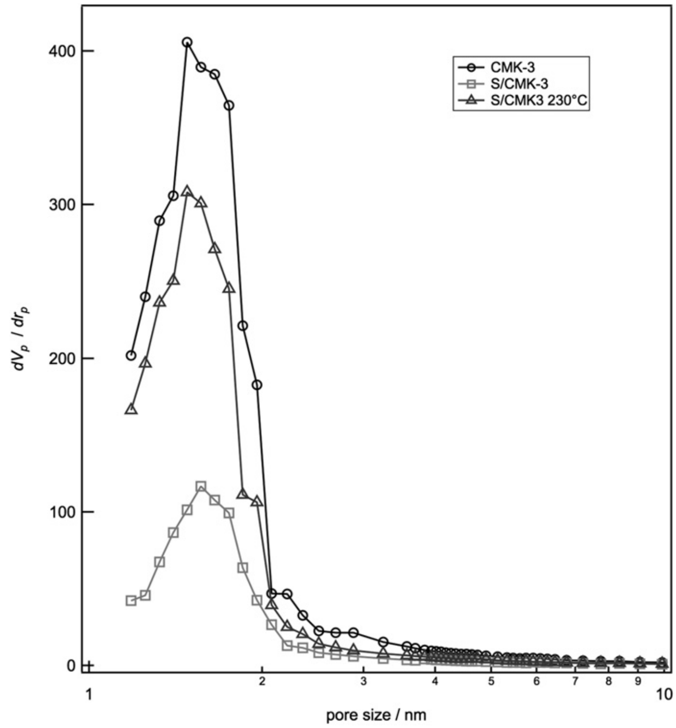

Fig. 3. Pore distributions of CMK-3, sulfur/CMK-3 composite, and a sample prepared by annealing at 230 °C.

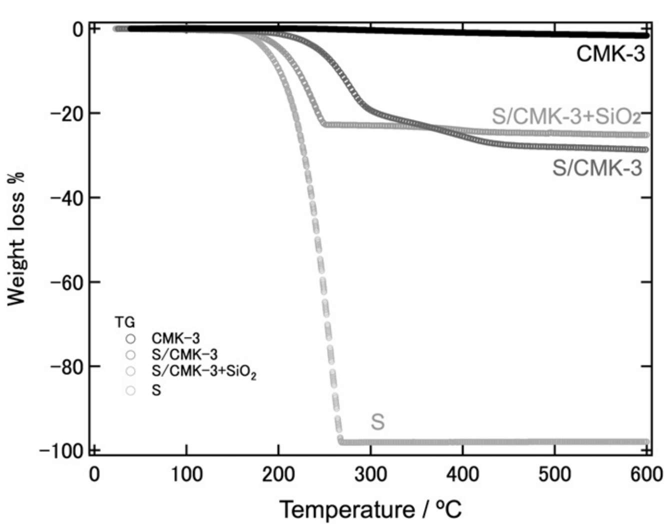

Fig. 2. TGA curves of CMK-3, sulfur, sulfur/CMK-3 composite, and sulfur/(CMK-3 + SiO_2) composite.

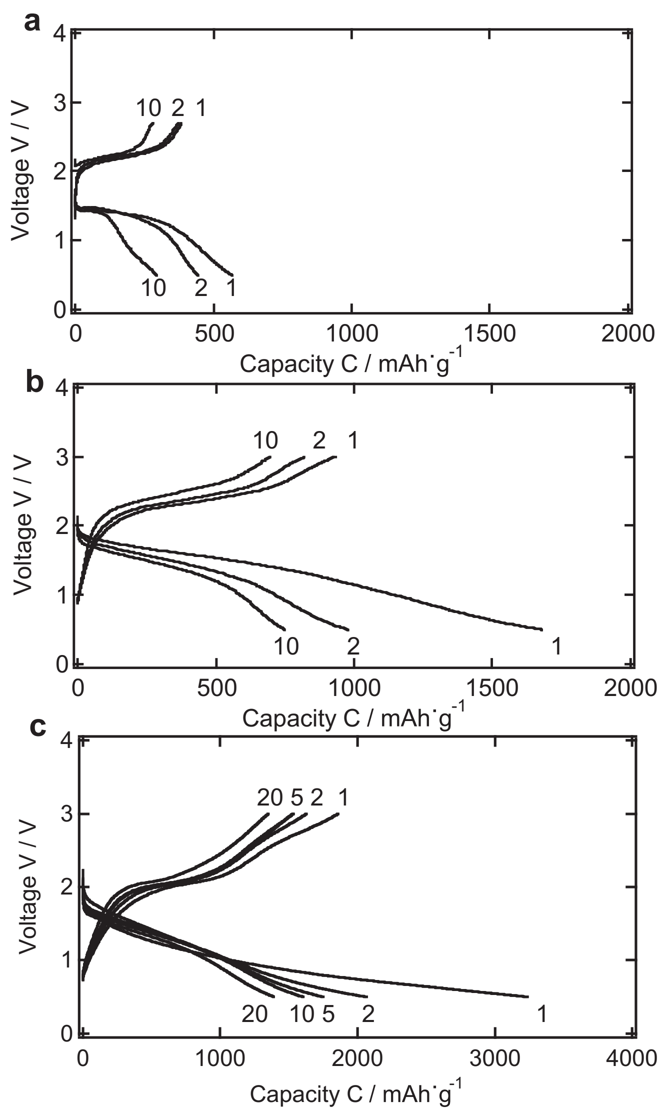

Fig. 4. Charge–discharge curves of all-solid-state batteries with composite electrodes of (a) sulfur/AB, (b) sulfur/CMK-3, and (c) sulfur/CMK-3 heat treated at 230 °C. Current density is 0.13 mA cm^{-2}.

that the carbon matrix also participates in the charge–discharge reactions of the composite electrode. The slightly lower cell voltages than those of conventional Li/S batteries [11] during the charge–discharge reaction also indicates an interaction between lithium and the carbon matrix. Fig. 6 shows the relationship between the capacity and the current density in the charge–discharge cycle. The first discharge capacity decreased with increasing current density. The capacity was 685 mAh g^{-1} at a current density of 1.3 mA cm^{-2}. Even after the fifth cycle, the capacity was 175 mAh g^{-1}. The composite electrode made it possible to realize a very high current density in the elemental sulfur electrode.

The large reduction in the capacity with cycling in Fig. 4 may be due to sulfur attached to the surfaces of carbon particles. Large volume changes of sulfur during cycling with a reaction between S and Li_2S may reduce the electronic contact, resulting in a large capacity loss. Removing sulfur from the particles improved the charge–discharge characteristics.

Since the maximum sulfur/carbon ratio in the sulfur/composite electrodes was calculated to be 76.3 wt.% based on the pore volume of CMK-3 (1.56 cm^3 g^{-1}) and the density of α-sulfur (2.069 g cm^{-3}), electrodes with sulfur ratios of 30, 50, and 70 wt.% were synthesized. Electrodes containing 30, 50, and 70 wt.% sulfur had first discharge capacities of 786, 1068, and 347 mAh g^{-1}, respectively. This indicates that the sulfur content of 50 wt.% gave the highest sulfur utilization. The thermal characteristics of these composite electrodes were investigated by TGA, as shown in Fig. 7. Sulfur/carbon composites containing 50 and 70 wt.% sulfur exhibited three weight losses; a third weight loss appeared between the two observed for the 30 wt.% sulfur composite electrode. The first weight loss corresponds to sulfur loss outside the pores, while the second and third weight losses are due to sulfur loss inside the pores. Table 1 lists the ratios of sulfur inside and outside of the

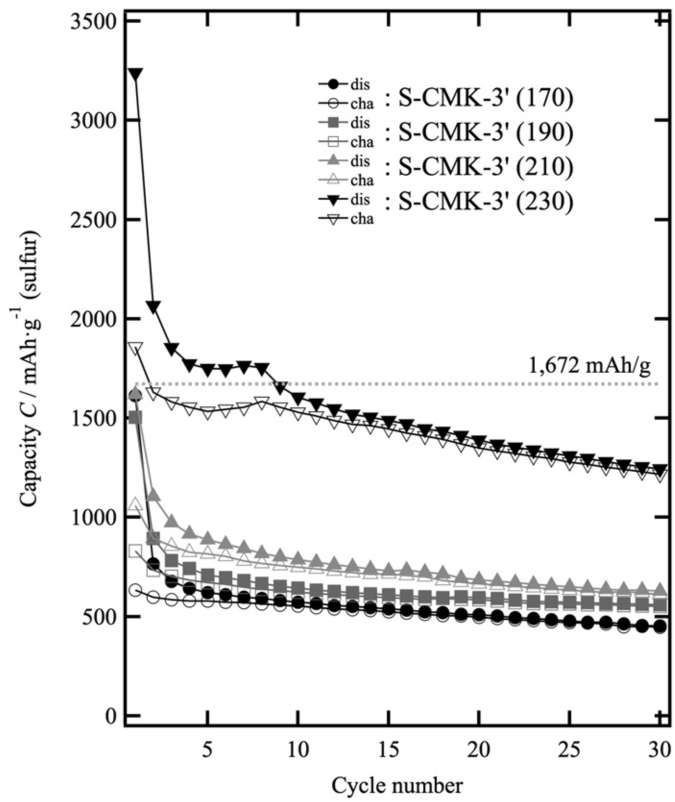

Fig. 5. Charge–discharge capacities as a function of cycle number for sulfur/CMK-3 composite annealed at various temperatures.

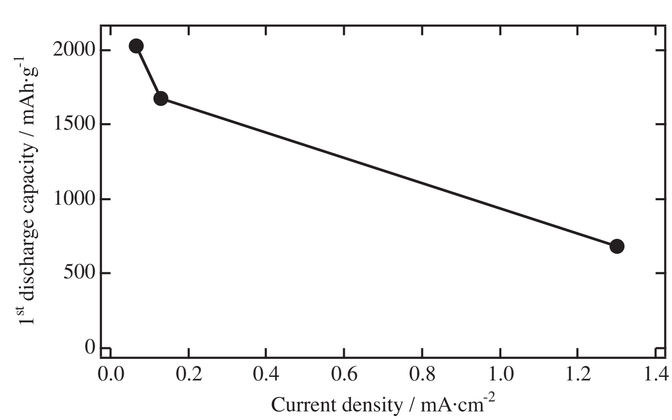

Fig. 6. Rate dependence of the first discharge capacity of the cell with sulfur/CMK-3 composite electrode.

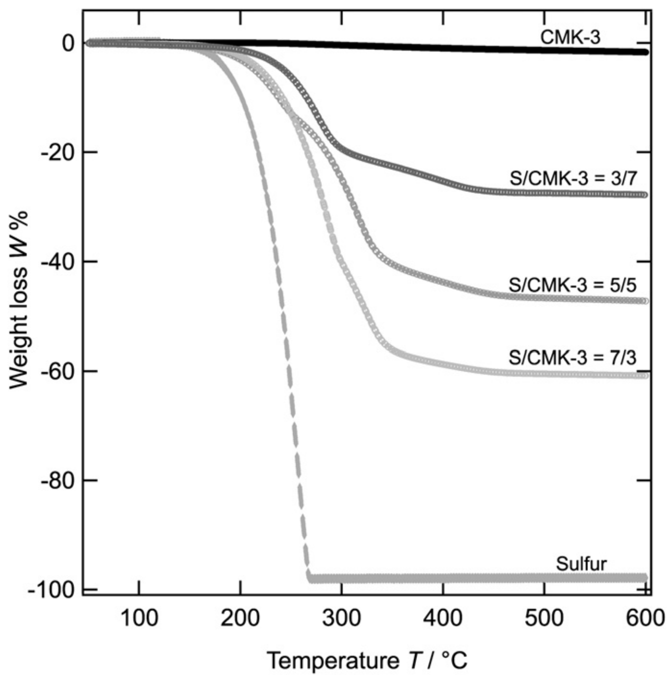

Fig. 7. TGA curves for sulfur/CMK-3 composites with a sulfur/CMK-3 ratio of 3/7, 5/5, and 7/3.

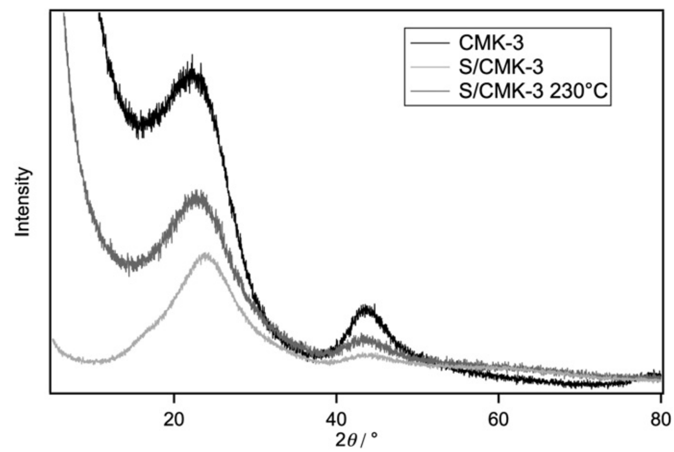

Fig. 8. X-ray diffraction patterns of CMK-3, S/CMK-3 composite, and S/CMK-3 composite after annealing at 230 °C.

Table 2
Crystallite size, L (Å), and d-values (Å) calculated from broadening of X-ray diffraction peak for CMK-3, S/CMK-3, and S/CMK-3 after annealing at 230 °C.

	d_{002}	d_{100}	$L_{C\ 002}$	$L_{C\ 001}$	$L_{C\ 100}$
CMK-3	3.79	2.05	9.8 (four sheets)	3.9	16.3 (nine units)
S/CMK-3	3.74	2.02	7.6 (three sheets)	–	11.5 (seven units)
S/CMK-3(230 °C)	3.83	2.04	10.0 (four sheets)	2.9	16.9 (10 units)

pores in CMK-3. The composite containing 50 wt.% sulfur (S/C = 5/5) had the smallest amount of sulfur outside of the pores and the highest amount of sulfur inside the pores. The composite containing 70 wt.% of sulfur (S/C = 7/3) had more sulfur inside the pores than the composite with 30 wt.% of sulfur (S/C = 3/7). The difference in the first discharge capacities of these composites depends on the amount of sulfur outside the pores. TGA curves of samples heated at 230 °C for 5 h reveal a third weight loss; this indicates that the sulfur evaporated in the third step exists near the carbon rod and may interact strongly with the carbon. The sulfur evaporated in the second step corresponds to that in the pore centers. The first discharge capacities for S/C = 3/7, 5/5, and 7/3 are 3239, 3146, and 3608 mAh g^{-1}, respectively. The high first discharge capacities, which exceed the theoretical capacity, may be caused by a reaction between lithium and sulfur inside the pore. Furthermore, a reaction between lithium and sulfur may also contribute to this high capacity.

Fig. 8 shows X-ray diffraction patterns of CMK-3, S/CMK-3 composite, and S/CMK-3 after annealing at 230 °C. The 002 peak shifts on mixing, whereas no peak shifts were observed for the 100 reflection. Table 2 lists d-values, and the crystallite size, L, calculated from the peak broadening for CMK-3, S/CMK-3 composite, and S/CMK-3 after annealing at 230 °C. d changes with mixing and annealing, which indicates that sulfur interacts with the carbon structure during heating. The changes in the distance between adjacent carbon layers indicate an interaction between the sulfur. The strength of this interaction may increase with increasing heating temperature. The amount of sulfur inside the carbon layer increases with the heating temperature. The peak at about 11° corresponds to the 001 reflection. It disappeared after sulfur mixing. This indicates that mixing orders the stacking along the c-axis. The absence of any shift in the 100 reflection peak indicates that no structural changes occurred in the ab plane of the graphene layers and the broadening of this peak suggests an increase in the number of edges of graphene layers. A strong interaction between the sulfur and the edges of the carbon layers is responsible for the lattice space changes in the carbon nanocrystals. The sulfur at the edges of the carbon rod also forms a close contact with the solid electrolyte during milling when preparing the electrode. This results in the high performance of the charge–discharge reaction. The sulfur attached to the carbon rod after heat treatment connects with the solid electrolyte after mixing, which provides the electrode structure with good charge–discharge characteristics. The charge–discharge reaction mechanism may differ from those observed for a Li/S cell with a liquid electrolyte, which might provide new possibilities for all-solid-state Li/S cells. Further investigation of the reaction mechanism by small-angle X-ray scattering is currently in progress.

Table 1
Ratio of sulfur inside and outside pores for composites electrodes.

S/CMK-3	Weight percent of sulfur		
	Total	Outside pores	Inside pores
3/7	27.8	18.4	9.4
5/5	47.2	12.9	34.3
7/3	60.8	39.1	21.7

4. Summary

All-solid-state cells with an S/CMK-3 composite electrode and a thio-LISICON electrolyte exhibit a high electrode capacity and charge–discharge reversibility. Sulfur was introduced into mesopores between carbon rods. Additional sulfur attached to the surfaces of the carbon particles was removed by annealing at 230 °C. Mixing with sulfur results in sulfur interacting with the graphene sheets of the carbon matrix. As the high charge–discharge capacities of the electrodes were calculated based on the weight of sulfur in the electrode matrix, the carbon matrix may also participate in the charge–discharge cycles, which causes the slightly higher discharge voltage of about 1.5 V vs. LiAl negative

electrodes. The excess capacity may also be due to lithium being incorporated in the carbon matrix. Although the mechanism of the sulfur electrodes remains unclear, sulfur exhibited a relatively high reversibility during charge–discharge cycles and the composite structure of sulfur and carbon is found to be very effective for all-solid-state lithium–sulfur batteries.

Acknowledgment

This work is supported by the Li-ion and Excellent Advanced Batteries Development (Li-EAD) Project of the New Energy and Industrial Technology Department Organization (NEDO), Japan.

References

[1] J.A. Dean, Lange's Handbook of Chemistry. McGraw-Hill, New York, 1985, pp. 3–5.
[2] D. Marmorstein, T.H. Yu, K.A. Striebel, F.R. McLarnon, J. Hou, E.J. Cairns, J. Power Sources 89 (2000) 219–226.
[3] H. Yamin, E. Peled, J. Power Sources 9 (1983) 281–287.
[4] R.D. Rauh, K.M. Abraham, G.F. Pearson, J.K. Surprenant, S.B. Brummer, J. Electrochem. Soc. 126 (1979) 523–527.
[5] J. Shim, K.A. Striebel, E.J. Cairns, J. Electrochem. Soc. 149 (2002) A1321–A1325.
[6] L. Wang, S. Lin, K. Lin, C. Yin, D. Liang, Y. Di, P. Fan, D. Jiang, F.-S. Xiao, Microporous Mesoporous Mater. 85 (2005) 136–142.
[7] A.B. Fuertes, S. Alvarez, Carbon 42 (2004) 3049–3055.
[8] P.M. Barata-Rodrigues, T.J. Mays, G.D. Moggridge, Carbon 41 (2003) 2231–2246.
[9] S. Han, M. Kim, T. Hyeon, Carbon 41 (2003) 1525–1532.
[10] S. Jun, S.H. Joo, R. Ryoo, M. Kruk, M. Jaroniec, Z. Liu, T. Ohsuna, O. Terasaki, J. Am. Chem. Soc. 122 (2000) 10712–10713.
[11] X. Ji, K.T. Lee, L.F. Nazar, Nat. Mater. 8 (2009) 500–506.
[12] R. Kanno, T. Tatsumi, T. Yokoi, M. Nagao, T. Kobayashi, R. Watanabe, Y. Imade, Jpn. Kokai Tokkyo Koho (2010), JP2010095390A.
[13] R. Kanno, M. Murayama, J. Electrochem. Soc. 148 (2001) A742–A746.
[14] T. Matsumura, K. Nakano, R. Kanno, A. Hirano, N. Imanishi, Y. Takeda, Journal of Power Sources, 13th International Meeting on Lithium Batteries, 174 (2007) 632–636.
[15] T. Kobayashi, Y. Imade, D. Shishihara, K. Homma, M. Nagao, R. Watanabe, T. Yokoi, A. Yamada, R. Kanno, T. Tatsumi, J. Power Sources 182 (2008) 621–625.
[16] Y. Imade, T. Kobayashi, M. Nagao, K. Homma, Y. Yamakawa, A. Yamada, R. Kanno, R. Watanabe, T. Yokoi, T. Tatsumi, The Chemical Society of Japan/Kanto Branch, Kiryu, Japan (2008). 2P-079.
[17] R. Kanno, M. Murayama, T. Inada, T. Kobayashi, K. Sakamoto, N. Sonoyama, A. Yamada, S. Kondo, Electrochem. Solid-State Lett. 7 (2004) A455–A458.
[18] E.P. Barrett, L.G. Jpyner, P.P. Halenda, J. Am. Chem. Soc. 73 (1951) 373–380.